

Gyrokinetic Stability of Electron-Positron-Ion Plasmas

A. Mishchenko¹†, A. Zocco¹, P. Helander¹, and A. Könies¹

¹Max Planck Institute for Plasma Physics, D-17491 Greifswald, Germany

(Received xx; revised xx; accepted xx)

The gyrokinetic stability of electron-positron plasmas contaminated by ion (proton) admixture is studied in slab geometry. The appropriate dispersion relation is derived and solved. The ion-temperature-gradient driven instability, the electron-temperature-gradient driven instability, the universal mode, and the shear Alfvén wave are considered. The contaminated plasma remains stable if the contamination degree is below some threshold, and it is found that the shear Alfvén wave can be present in a contaminated plasma in cases where it is absent without ion contamination.

1. Introduction

The prospects of creating electron-positron pair plasmas magnetically confined in dipole or stellarator geometries have been discussed since early 2000's (Pedersen *et al.* 2003). In near future, the first experiment aiming at this goal will be constructed (Pedersen *et al.* 2012). Recently, efficient injection and trapping of a cold positron beam in a dipole magnetic field configuration has been demonstrated by Saitoh *et al.* (2015). This result is a key step towards the ultimate aim of creating and studying of the first man-made magnetically-confined pair plasma in the laboratory.

It has been shown by Helander (2014) that pair plasmas possess unique gyrokinetic stability properties thanks to the mass symmetry between the particle species. For example, drift instabilities are completely absent in straight unshered geometry, e. g. in a slab. They can be destabilised only in the presence of magnetic curvature in more complicated confining fields. Helander & Connor (2016) found that this result persists also in the electromagnetic regime. But, what happens if the perfect mass symmetry between the positively charged particles (positrons) and the negatively charged ones (electrons) is broken? This can happen if some fraction of ions (e. g. protons) is introduced into the pair plasma, which probably will be the case in experiments since the pumping and vacuum systems are never completely perfect. Then one could expect that the drift instabilities will reappear.

In this paper, we address the effect of proton contamination on the gyrokinetic stability of pair plasmas. We find that drift instabilities can indeed appear in contaminated pair plasmas if the proton fraction exceeds some threshold. Also, we find that the shear Alfvén wave is present in contaminated plasma even if the ion contamination is small. Its frequency, however, increases rapidly when the ion fraction becomes negligible.

The structure of the paper is as follows. In §2, the general electromagnetic dispersion relation is derived. It describes slab gyrokinetic stability in plasmas with an arbitrary number of species, although we consider only three species in this work. In §3, the stable part of the gyrokinetic spectrum is addressed. In §4, §5 and §6, drift instabilities in three-

† Email address for correspondence: alexey.mishchenko@ipp.mpg.de

component plasmas are considered. In §7, the shear Alfvén wave in electron-positron-ion plasmas is described. Conclusions are summarised in §8.

2. Dispersion relation

Following Helander (2014) and Helander & Connor (2016), we use gyrokinetic theory to analyse the linear stability of electron-positron-ion plasmas. It is convenient to write the gyrokinetic distribution function in the form:

$$f_a = f_{a0} \left(1 - \frac{e_a \phi}{T_a} \right) + g_a = f_{a0} + f_{a1}, \quad f_{a1} = -\frac{e_a \phi}{T_a} f_{a0} + g_a \quad (2.1)$$

Here, f_{a0} is a Maxwellian, a is the species index with $a = e$ corresponding to electrons, $a = p$ to positrons, and $a = i$ to the ions. The linearised gyrokinetic equation in this notation is

$$i v_{\parallel} \nabla_{\parallel} g_a + (\omega - \omega_{da}) g_a = \frac{e_a}{T_a} J_0 \left(\frac{k_{\perp} v_{\perp}}{\omega_{ca}} \right) (\omega - \omega_{*a}^T) (\phi - v_{\parallel} A_{\parallel}) f_{a0} \quad (2.2)$$

with J_0 the Bessel function, ω_{ca} the cyclotron frequency, k_{\perp} the perpendicular wave number, ϕ the perturbed electrostatic potential and A_{\parallel} the perturbed parallel magnetic potential in the Coulomb gauge. Other notation used is

$$\omega_{*a}^T = \omega_{*a} \left[1 + \eta_a \left(\frac{v^2}{v_{\text{tha}}^2} - \frac{3}{2} \right) \right], \quad v = \sqrt{v_{\parallel}^2 + v_{\perp}^2}, \quad k_{\perp} = \sqrt{k_x^2 + k_y^2} \quad (2.3)$$

$$\omega_{*a} = \frac{k_y T_a}{e_a} \frac{d \ln n_a}{d \psi}, \quad \eta_a = \frac{d \ln T_a}{d \ln n_a}, \quad v_{\text{tha}} = \sqrt{\frac{2 T_a}{m_a}}, \quad \omega_{da} = \mathbf{k}_{\perp} \cdot \mathbf{v}_{da} \quad (2.4)$$

Here, the sign convention is such that $\omega_{*i} \leq 0$, $\omega_{*p} \leq 0$, and $\omega_{*e} \geq 0$. For simplicity we will assume $k_x = 0$ and $k_{\perp} = k_y$ throughout the paper. In slab geometry, $\omega_{da} = 0$. Taking the Fourier transform along the parallel coordinate, we obtain:

$$(\omega - k_{\parallel} v_{\parallel}) g_a = \frac{e_a}{T_a} J_0 \left(\frac{k_{\perp} v_{\perp}}{\omega_{ca}} \right) (\omega - \omega_{*a}^T) (\phi - v_{\parallel} A_{\parallel}) f_{a0} \quad (2.5)$$

This equation is trivially solved:

$$g_a = \frac{\omega - \omega_{*a}^T}{\omega - k_{\parallel} v_{\parallel}} \frac{e_a f_{a0}}{T_a} J_0 (\phi - v_{\parallel} A_{\parallel}) \quad (2.6)$$

The gyrokinetic quasineutrality condition and the parallel Ampere's law are

$$\left(\sum_a \frac{n_a e_a^2}{T_a} + \epsilon_0 k_{\perp}^2 \right) \phi = \sum_a e_a \int g_a J_0 d^3 v, \quad A_{\parallel} = \frac{\mu_0}{k_{\perp}^2} \sum_a e_a \int v_{\parallel} g_a J_0 d^3 v \quad (2.7)$$

For the electromagnetic dispersion relation, it is convenient to define:

$$W_{na} = -\frac{1}{n_a v_{\text{tha}}^n} \int \frac{\omega - \omega_{*a}^T}{\omega - k_{\parallel} v_{\parallel}} J_0^2 f_{a0} v_{\parallel}^n d^3 v \quad (2.8)$$

Taking velocity-space integrals, one finds:

$$W_{na} = \zeta_a \left\{ \left(1 - \frac{\omega_{*a}}{\omega} \right) Z_{na} \Gamma_{0a} + \frac{\omega_{*a} \eta_a}{\omega} \left[\frac{3}{2} Z_{na} \Gamma_{0a} - Z_{na} \Gamma_{*a} - Z_{n+2,a} \Gamma_{0a} \right] \right\} \quad (2.9)$$

Here, the following notation is employed:

$$\frac{1}{\lambda_{Da}^2} = \frac{q_a^2 n_a}{\epsilon_0 T_a}, \quad \frac{1}{\lambda_D^2} = \sum_a \frac{1}{\lambda_{Da}^2}, \quad b_a = k_{\perp}^2 \rho_a^2, \quad \rho_a = \frac{\sqrt{m_a T_a}}{|q_a| B} \quad (2.10)$$

$$\Gamma_{*a} = \Gamma_{0a} - b_a [\Gamma_{0a} - \Gamma_{1a}], \quad \Gamma_{0a} = I_0(b_a) e^{-b_a}, \quad \Gamma_{1a} = I_1(b_a) e^{-b_a} \quad (2.11)$$

$$Z_{na} = \frac{1}{\sqrt{\pi}} \int_{-\infty}^{\infty} \frac{x^n e^{-x^2} dx}{x - \zeta_a}, \quad \zeta_a = \frac{\omega}{k_{\parallel} v_{tha}} \quad (2.12)$$

Using this notation, we can cast the field equations into the form:

$$\left(1 + k_{\perp}^2 \lambda_D^2\right) \phi + \sum_a \frac{\lambda_D^2}{\lambda_{Da}^2} \left(W_{0a} \phi - W_{1a} A_{\parallel} v_{tha}\right) = 0 \quad (2.13)$$

$$A_{\parallel} + \frac{1}{c^2} \sum_a \frac{v_{tha}}{k_{\perp}^2 \lambda_{Da}^2} \left(W_{1a} \phi - W_{2a} A_{\parallel} v_{tha}\right) = 0 \quad (2.14)$$

Computing the determinant of this system of equations, we find the electromagnetic dispersion relation describing electron-positron-ion plasma in slab geometry:

$$\begin{aligned} & \left(1 + k_{\perp}^2 \lambda_D^2 + \sum_a \frac{\lambda_D^2}{\lambda_{Da}^2} W_{0a}\right) \left(1 - 2 \sum_a \frac{\beta_a}{k_{\perp}^2 \rho_a^2} W_{2a}\right) + \\ & + 2 \sum_a \frac{\lambda_D^2}{\lambda_{Da}^2} W_{1a} v_{tha} \sum_a \frac{\beta_a}{k_{\perp}^2 \rho_a^2} \frac{W_{1a}}{v_{tha}} = 0 \end{aligned} \quad (2.15)$$

Here, $\beta_a = \mu_0 n_a T_a / B^2$. The electrostatic limit corresponds, as usual, to $\beta_a = 0$.

In the following, we will use this dispersion relation in order to describe instabilities which can appear in three-component plasmas. This will give us insight into the general properties of the gyrokinetic stability of such plasmas.

3. Gyrokinetic stable modes

We first consider the case of a pure electrostatic electron-positron plasma. Assuming quasineutrality $\omega_{*p} = -\omega_{*e}$, equal temperatures $T_p = T_e$, and equal temperature gradients $\eta_p = \eta_e$, we can reduce the dispersion relation to

$$1 + k_{\perp}^2 \lambda_D^2 + \zeta Z_0 = 0 \quad (3.1)$$

Equations of this type have been considered in detail by (Fried & Gould 1961; Yegorenkov & Stepanov 1987, 1988) for conventional (hydrogen) plasmas. In a hydrogen plasma, equation (3.2), similar to Eq. (3.1), describes the plasma stability in the absence of the density and temperature gradients and assuming $T_i = T_e$:

$$1 + k_{\perp}^2 \lambda_D^2 + \frac{1}{2} [\zeta_i Z_0(\zeta_i) \Gamma_{0i} + \zeta_e Z_0(\zeta_e) \Gamma_{0e}] = 0 \quad (3.2)$$

This equation has an infinite number of solutions, called *K-modes* (Yegorenkov & Stepanov 1987, 1988). These modes can be of the ion type with $\zeta_i \geq 1$ or the electron type with $\zeta_e \geq 1$. In Fig. 1, the spectrum resulting from Eq. (3.2) for the conventional plasma is plotted including K-modes of the ion type. This spectrum was computed numerically using the Nyquist technique (Carpentier & Santos 1982; Davies 1986). The staircase-like visual appearance of Figs. 1 and 2 is an artefact caused by the density of the roots of

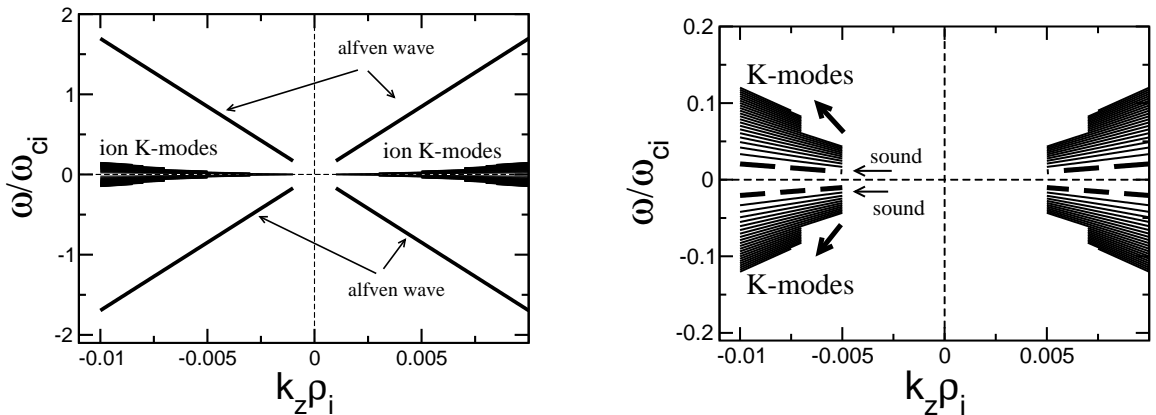


FIGURE 1. Left: gyrokinetic frequency spectrum for conventional plasmas including sound and Alfvén waves. Right: low-frequency part of the spectrum.

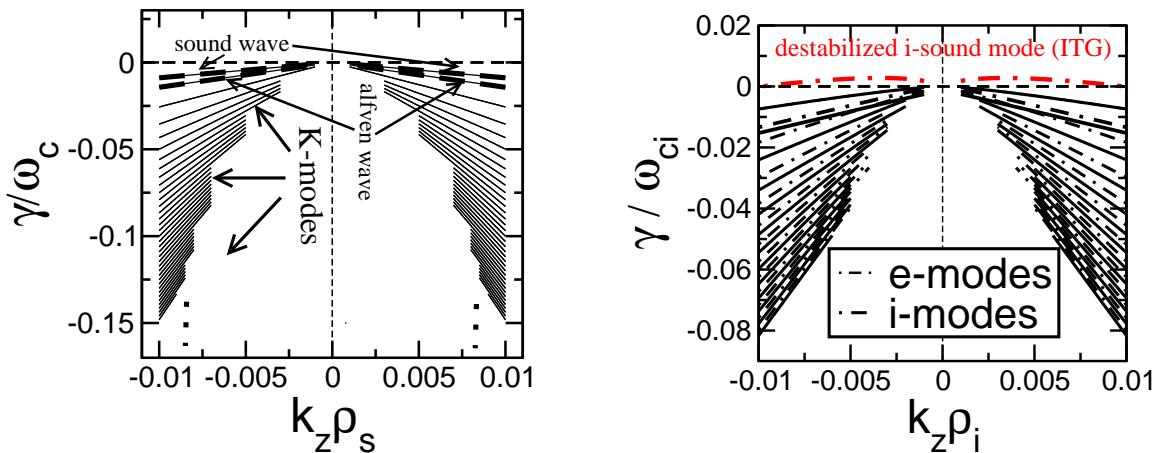


FIGURE 2. Left: the imaginary part of the spectrum in a homogeneous plasma. Right: the same in the presence of an ion temperature gradient $\kappa_{Ti} = 0.1$. In this Figure, i-modes denote modes rotating in the ion diamagnetic direction and e-modes correspond to modes rotating in the electron diamagnetic direction.

the dispersion relation increasing towards the origin of the coordinates. This complicates the numerical solution in this area.

In Fig. 2, one sees that, as Fried & Gould (1961) suggested, most of the solutions of Eq. (3.2) are strongly damped, satisfying $|\gamma| \sim |\omega|$. The least damped solutions can be destabilised by plasma profile gradients leading either to the Ion Temperature Gradient driven instability (ITG), or the Electron Temperature Gradient driven instability (ETG), or the universal instability, driven by the density gradient. This is shown in Fig. 2, where the effect of the ion temperature gradient on the gyrokinetic spectrum in a conventional plasma can be seen. In pure pair plasmas, however, the electron and the positron diamagnetic contributions cancel also in presence of profile gradients, making

such plasmas absolutely stable in slab geometry within the gyrokinetic description. Note however, that perfect symmetry between the electron and positron density and temperature profiles is required to guarantee the cancellation of the diamagnetic terms. While density profiles are always identical for the two species in a quasineutral plasma, the temperature profiles can differ. In this case, a pure pair plasma can be temperature-gradient unstable, as we will see in the following. The gradient-driven instabilities can also appear if a pair plasma is “contaminated” by protons or other ions.

Some analytic progress can be made for K-modes in an electron-positron plasma. Assuming $\zeta_e = \zeta_p \gg 1$ and $\gamma \sim \omega$, the plasma dispersion function can be approximated:

$$Z_0(\zeta_e) \approx 2i\sqrt{\pi}e^{-\zeta_e^2} - \frac{1}{\zeta_e} - \frac{1}{2\zeta_e^3} \quad (3.3)$$

For this expansion, the dispersion relation takes the form:

$$4i\sqrt{\pi}\zeta_e^3 e^{-\zeta_e^2} = 1 \quad (3.4)$$

Introducing the notation $\zeta_e = x - iy$ and assuming $x = \pm(y + \Delta)$ with $\Delta \ll y$ (Yegorenkov & Stepanov 1987, 1988), we can write the dispersion relation in the form:

$$8y^3\sqrt{2\pi}e^{-2y\Delta} \exp(2iy^2 - i\pi/4) = 1 \equiv \exp(2\pi mi) \quad (3.5)$$

Splitting this relation into equations for the argument and for the absolute value and employing $\Delta/y \ll 1$, we obtain:

$$2y^2 - \pi/4 = 2\pi m, \quad 8y^3\sqrt{2\pi}e^{-2y\Delta} = 1 \quad (3.6)$$

Thus, an infinite family of solutions is found:

$$y_m = \sqrt{\pi m + \pi/8} \approx \sqrt{\pi m}, \quad \Delta_m = \frac{\ln(8y_m^3\sqrt{2\pi})}{2y_m}, \quad x_m = \pm(y_m + \Delta_m) \quad (3.7)$$

Finally, we write our solutions in the form:

$$\omega_m = \pm k_{\parallel} v_{\text{the}} x_m, \quad \gamma_m = -k_{\parallel} v_{\text{the}} y_m \quad (3.8)$$

These relations describe strongly-damped K-modes in a pure electron-positron plasma. In Fig. 3, we compare these analytic results with the numerical solution of the original dispersion relation Eq. (2.15) and find very good agreement. Note that the expansion Eq. (3.3) is valid for $m \gg 1$. For low m , the dispersion relation must be solved numerically.

In a conventional plasma, one can make the usual assumption $\zeta_i \gg 1$ and $\zeta_e \ll 1$. In this case, the following expansions can be used:

$$Z_0(\zeta_i) = 2i\sqrt{\pi}e^{-\zeta_i^2} - \frac{1}{\zeta_i} - \frac{1}{2\zeta_i^3}, \quad Z_0(\zeta_e) = i\sqrt{\pi} - 2\zeta_e \quad (3.9)$$

which lead to the approximated dispersion relation:

$$(1 - \Gamma_{0i}/2) + \left(i\zeta_i\sqrt{\pi}e^{-\zeta_i^2} - \frac{1}{4\zeta_i^2} \right) \Gamma_{0i} + \mathcal{O}(\zeta_e) = 0 \quad (3.10)$$

For simplicity, we neglect Finite Larmor Radius (FLR) effects, implying $\Gamma_{0i} = 1$. Also, the small contribution $1/(4\zeta_i^2) \ll 1$ can be neglected compared to the other terms. Then, we obtain:

$$2i\zeta_i\sqrt{\pi}e^{-\zeta_i^2} + 1 = 0 \quad (3.11)$$

Using the notation $\zeta_i = x - iy$ with $x = \pm(y + \Delta)$ and employing $\Delta \ll 1$, we can split

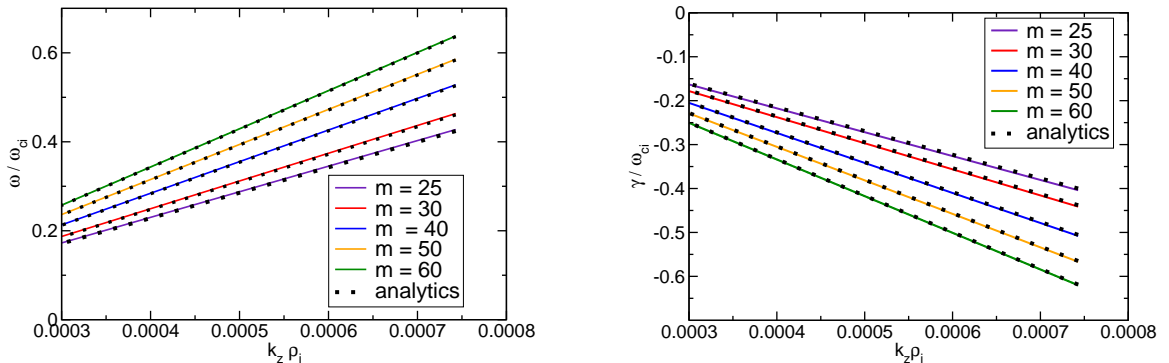


FIGURE 3. “K-mode” solution of the dispersion relation for a pure pair plasma. All modes are strongly damped. Here, $k_{\perp}\lambda_D = 0$ has been assumed. The numerical solution of Eq. (2.15) is compared with the analytic result Eq. (3.8).

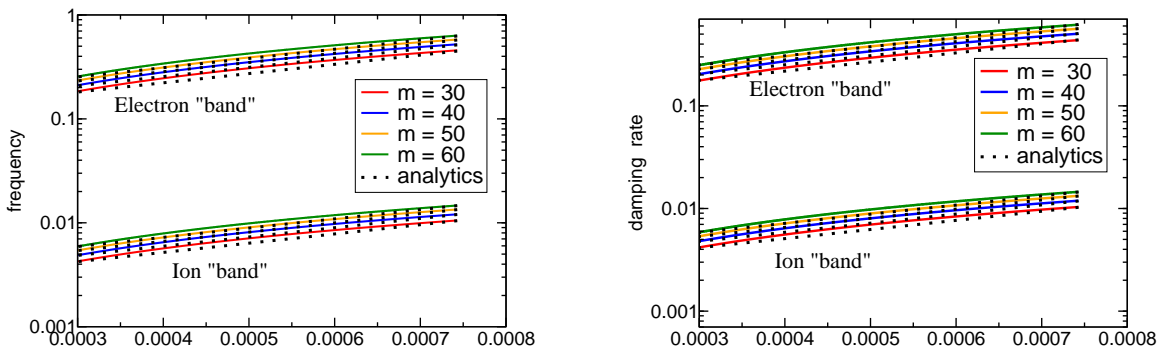


FIGURE 4. “K-mode” solution of the dispersion relation for conventional plasma assuming $k_{\perp}\lambda_D = 0$. One can see the ion and the electron parts of the spectrum. The numerical solution of Eq. (2.15) is compared with the analytic result Eq. (3.13).

the dispersion relation into equations for the argument and for the absolute value:

$$2y\sqrt{2\pi}e^{-2y\Delta} \exp(2iy^2 - 3\pi i/4) = 1 \equiv \exp(2\pi mi) \quad (3.12)$$

Finally, the solutions for the K-modes of the ion type are

$$y_m = \sqrt{\pi m + \frac{3\pi}{8}} \approx \sqrt{\pi m}, \quad \Delta_m = \frac{\ln(2y\sqrt{2\pi})}{2y}, \quad x_m = y_m + \Delta_m \quad (3.13)$$

In Fig. 4, these analytic results are compared with the numerical solution of the original (exact) dispersion relation Eq.(2.15).

Interestingly, the same dispersion relation can be obtained for K-modes in a pure pair plasma keeping the Debye length finite. In this case, the dispersion relation Eq. (3.4) is replaced by

$$4i\sqrt{\pi}\zeta_e^3 e^{-\zeta_e^2} + 2\zeta_e^2 k_{\perp}^2 \lambda_D^2 = 1 \implies 2i\sqrt{\pi}\zeta_e e^{-\zeta_e^2} + k_{\perp}^2 \lambda_D^2 = 0 \quad (3.14)$$

which reduces to Eq. (3.11) if $k_{\perp}\lambda_D \gg 1/\zeta_e$ with $k_{\perp}\lambda_D$ replacing 1 and ζ_e replacing ζ_i .

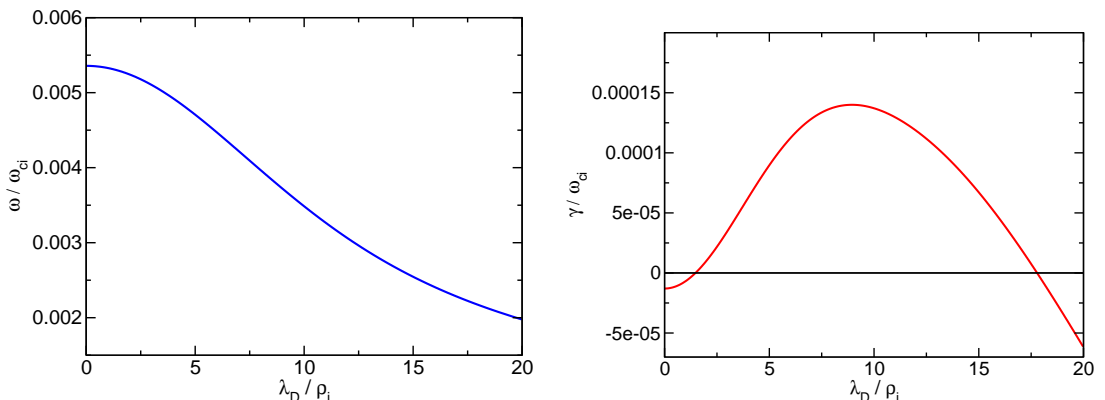


FIGURE 5. Frequency and growth rate of the universal mode as functions of the Debye length in a contaminated pair plasma with the positron fraction $\nu_p = 0.7$. The parameters are $k_{\perp}\rho_i = 0.1$, $k_{\parallel}\rho_i = 7.43 \times 10^{-4}$, $\kappa_{ni}\rho_i = \kappa_{ne}\rho_i = \kappa_{np}\rho_i = 0.3$, and $\kappa_{Ti}\rho_i = \kappa_{Te}\rho_i = \kappa_{Tp}\rho_i = 0.0$ with $\kappa_{na} = d \ln n_a / d \ln x$ and $\kappa_{Ta} = d \ln T_a / d \ln x$.

In a hydrogen plasma, a dispersion relation, very similar to Eq. (3.11), can be obtained assuming $\zeta_e \gg 1$:

$$\frac{1 - \Gamma_{0i}}{2} + \left(i\zeta_e \sqrt{\pi} e^{-\zeta_e^2} - \frac{1}{4\zeta_e^2} \right) + \mathcal{O}\left(\frac{1}{\zeta_e^2}\right) = 0 \quad (3.15)$$

Here, recall that $\zeta_i \gg \zeta_e$. This dispersion relation coincides with the ion K-mode dispersion relation Eq. (3.11) at finite $k_{\perp}\lambda_D$, and transforms into the pair-plasma K-mode dispersion relation without $k_{\perp}\lambda_D$, see Eq. (3.4), when $k_{\perp} \rightarrow 0$.

In a three-component plasma with the ion fraction $\nu_i = n_i/n_e$, the K-mode dispersion relation for $\zeta_e \gg 1$ becomes

$$\nu_i(1 - \Gamma_{0i}) + (2 - \nu_i) \left(2i\zeta_e \sqrt{\pi} e^{-\zeta_e^2} - \frac{1}{2\zeta_e^2} \right) + \mathcal{O}\left(\frac{1}{\zeta_e^2}\right) = 0 \quad (3.16)$$

The last term ($\sim 1/\zeta_e^2$) is negligible unless $\nu_i \rightarrow 0$ or $k_{\perp} \rightarrow 0$. Here, electron and positron FLR effects have been neglected.

In summary, K-modes, considered in this Section, are the only solutions of the slab dispersion relation in pure electron-positron plasma for arbitrary density and temperature profiles provided these profiles coincide for the two species. If the positron and the electron temperature profiles differ, a temperature-driven instability can appear also for pure pair plasma in slab geometry. This will be considered in more detail in the following.

4. Universal instability

The first unstable mode to be considered is the universal instability driven by the density gradient. For simplicity, we assume the temperature profiles to be flat. In this case, the dispersion relation is

$$1 + k_{\perp}^2 \lambda_D^2 + \frac{1}{2} \sum_{a=i,p,e} \nu_a \zeta_a \left(1 - \frac{\omega_{*a}}{\omega} \right) Z_{0s} \Gamma_{0s} = 0 \quad (4.1)$$

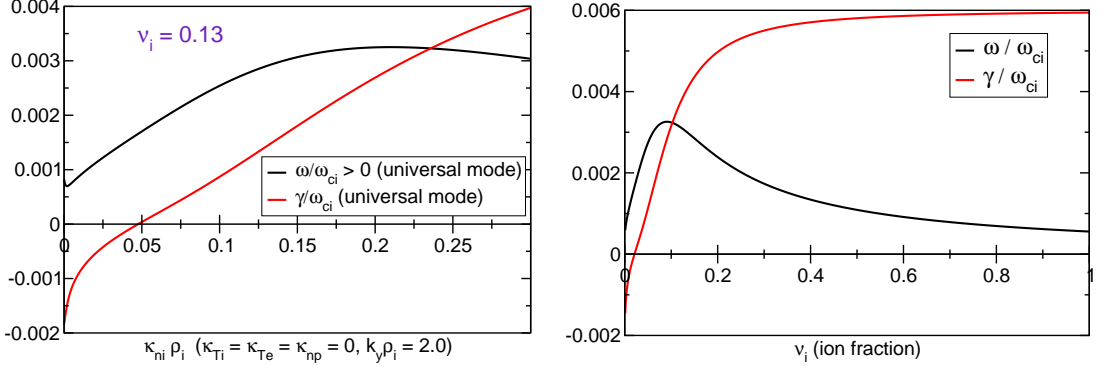


FIGURE 6. Frequency and growth rate of the universal mode in a contaminated pair plasma. One sees that the ion density gradient and the ion contamination must be larger than some threshold for the mode to become unstable. The ion density gradient $\kappa_{ni} \rho_i = 0.3$ has been used for the ν_i dependence (figure on the right).

Here, $\nu_a = n_a/n_e$ is the density fraction corresponding to a particular species $a = i, e, p$. For electrons, $\nu_e = 1$. Taking the limit $k_{\parallel} v_{thi} \ll \omega \ll k_{\parallel} v_{the}$, we obtain:

$$Z_{0i} \approx -\frac{1}{\zeta_i}, \quad Z_{1e} \approx i\sqrt{\pi} \quad (4.2)$$

To lowest order, the dispersion relation reduces to

$$\left[2(1 + k_{\perp}^2 \lambda_D^2) - \nu_i \Gamma_{0i} \right] \omega - \nu_i \omega_* \Gamma_{0i} + i \zeta_e \sqrt{\pi} \left[\omega(\nu_e + \nu_p) - \nu_i \omega_* \right] = 0 \quad (4.3)$$

Here, the notation $\omega_* = \omega_{*e} = -\omega_{*p}$ and quasineutrality, $\nu_e - \nu_p = \nu_i$, have been used. The electron and positron FLR have been neglected $\Gamma_{0e} = \Gamma_{0p} = 1$. We solve the dispersion relation for $\omega = \omega_r + i\gamma$ assuming $\omega_r \gg \gamma$. Then, to the lowest order,

$$\omega_r = \frac{\nu_i \omega_* \Gamma_{0i}}{2(1 + k_{\perp}^2 \lambda_D^2) - \nu_i \Gamma_{0i}}, \quad \gamma = 2\zeta_e \sqrt{\pi} \nu_i \omega_* \frac{k_{\perp}^2 \lambda_D^2 + (1 - \Gamma_{0i})}{[2(1 + k_{\perp}^2 \lambda_D^2) - \nu_i \Gamma_{0i}]^2} \quad (4.4)$$

One sees that in the long-wavelength limit, $\Gamma_{0i} \rightarrow 1$, the universal mode is unstable for finite $k_{\perp} \lambda_D$ with ω_r independent of λ_D and $\gamma \sim k_{\perp}^2 \lambda_D^2$ for small $k_{\perp}^2 \lambda_D^2$. For large $k_{\perp}^2 \lambda_D^2$, both ω_r and $\gamma \sim 1/k_{\perp}^2 \lambda_D^2$. This behaviour is seen in the numerical solution of the dispersion relation Eq. (2.15) shown in Fig. 5. Here, we use the parameters $k_{\perp} \rho_i = 0.1$, $k_{\parallel} \rho_i = 7.43 \times 10^{-4}$, $\kappa_{ni} \rho_i = \kappa_{ne} \rho_i = \kappa_{np} \rho_i = 0.3$, and $\kappa_{Ti} \rho_i = \kappa_{Te} \rho_i = \kappa_{Tp} \rho_i = 0.0$ with $\kappa_{na} = d \ln n_a / d \ln x$ and $\kappa_{Ta} = d \ln T_a / d \ln x$.

For $\lambda_D = 0$, the universal mode needs $k_{\perp} \rho_i \sim 1$ to be unstable. The numerical solution corresponding to this case is shown in Fig. 6. The dispersion relation (2.15) is solved for the parameters $k_{\perp} \rho_i = 2.0$, $k_{\parallel} \rho_i = 7.4 \times 10^{-4}$, $\kappa_{Ti} = \kappa_{Te} = 0$, $\lambda_D = 0$. One sees that the universal instability can exist in pair plasmas in slab geometry but requires both the proton fraction and the ion density gradient to exceed than some threshold. Practically, it suggests that the universal mode will be stable in pair plasmas if the proton contamination is small. Interestingly, the *positron* density gradient has zero effect on the universal mode if quasineutrality $n_e = n_p + n_i$ is assumed since any effect of the positron density gradient on the universal mode is perfectly cancelled by the electrons.

5. ITG instability

For simplicity, we consider the flat-density limit. In this case, it is convenient to define $\omega_{Ta} = \eta_a \omega_{*a}$ with $a = i, e, p$ being the species index. For electrons and positrons, we assume flat profiles $\omega_{Te} = \omega_{Tp} = 0$. For ions, the temperature gradient is finite $\omega_{Ti} \neq 0$. To allow for unequal temperatures of different species, we introduce the notation:

$$\hat{\nu}_a = \frac{2\nu_a/\tau_a}{\sum_{a'} \nu_{a'}/\tau_{a'}} \quad (5.1)$$

with $\nu_a = n_a/n_e$ and $\tau_a = T_a/T_e$. Note that quasineutral plasmas satisfy both $\sum_a \nu_a = 2$ and $\sum_a \hat{\nu}_a = 2$. If the temperatures of all species are equal ($\tau_a = 1$) in such plasmas, then $\hat{\nu}_a = \nu_a$. In our notation, the dispersion relation becomes

$$1 + k_{\perp}^2 \lambda_D^2 + \sum_{a=i,p,e} \frac{\hat{\nu}_a}{2} \zeta_a Z_{0a} \Gamma_{0a} + \frac{\hat{\nu}_i \omega_{Ti} \zeta_i}{2\omega} \left(\frac{3}{2} Z_{0i} \Gamma_{0i} - Z_{0i} \Gamma_{*i} - Z_{2i} \Gamma_{0i} \right) = 0 \quad (5.2)$$

We consider the long wave-length limit $\Gamma_{0a} = \Gamma_{*a} = 1$ for all particle species. For the ITG instability, we can assume $k_{\parallel} v_{thi} \ll \omega \ll k_{\parallel} v_{the}$. Then, the plasma dispersion function can be expanded as

$$Z_0(\zeta_i) \approx -\frac{1}{\zeta_i} - \frac{1}{2\zeta_i^3} - \frac{3}{4\zeta_i^5}, \quad Z_0(\zeta_p) = Z_0(\zeta_e) \approx i\sqrt{\pi} \quad (5.3)$$

To leading order, we obtain the dispersion relation

$$1 - \frac{\hat{\nu}_i}{2} + k_{\perp}^2 \lambda_D^2 = -\frac{\hat{\nu}_i \omega_{Ti}}{4\omega^3} k_{\parallel}^2 v_{thi}^2 \quad (5.4)$$

Noting that $\omega_{Ti} < 0$, we find the unstable solution of this dispersion relation:

$$\omega = \frac{1}{2^{1/3}} \left(\frac{\hat{\nu}_i |\omega_{Ti}| k_{\parallel}^2 v_{thi}^2}{2 - \hat{\nu}_i + 2k_{\perp}^2 \lambda_D^2} \right)^{1/3} \left(-\frac{1}{2} + i \frac{\sqrt{3}}{2} \right) \quad (5.5)$$

This root corresponds to the well-known fluid limit of the slab ITG instability (Coppi *et al.* 1967). Note that the ITG frequency is negative, as expected. One sees that in an ion-contaminated electron-positron plasma, the frequency and growth rate of the fluid ITG instability are proportional to $(\hat{\nu}_i |\omega_{Ti}|)^{1/3}$. Hence, pure pair plasmas with $\hat{\nu}_i = 0$ cannot support the slab ITG. Similarly to the frequency and the growth rate, the destabilisation threshold is also determined by the product $\hat{\nu}_i |\omega_{Ti}|$, and not just $|\omega_{Ti}|$ as is the case for conventional (e. g. hydrogen) plasmas. Numerical results demonstrating this prediction are shown in Fig. 7. Here, the dependence of the ITG frequency and the growth rate on the proton contamination is plotted. One sees that the absolute value of the frequency indeed decreases strongly at a smaller proton content, in agreement with the analytic result. One also sees that the mode is unstable only when the proton content exceeds some threshold, whose value depends on the ion temperature gradient. This is of practical interest since it indicates that the ITG modes may be stable at a large ion temperature gradient in ion-contaminated pair plasmas if the ion fraction is small enough.

Another aspect of practical interest for the pair-plasma experiment (Pedersen *et al.* 2012) is the effect of the Debye length on the microinstabilities. This effect is usually negligible for tokamak or stellarator plasmas, where the Debye length is much smaller than the ion gyro-radius. In the pair-plasma experiment, however, the Debye length is not expected to be very small and can become comparable to the proton gyroradius. This

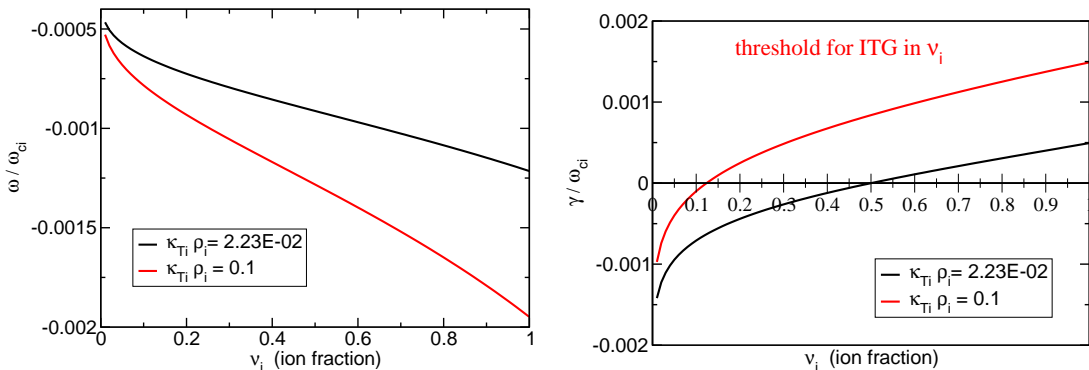


FIGURE 7. Effect of proton contamination on the ITG mode in a pair plasma. The wave numbers are $k_{\perp} \rho_i = 0.24$ and $k_{\parallel} \rho_i = 7.4 \times 10^{-4}$. The density and the electron temperature profiles are flat, $\kappa_{Ti} = d \ln T_i(x)/d \ln x$, and $\tau_i = 1$.

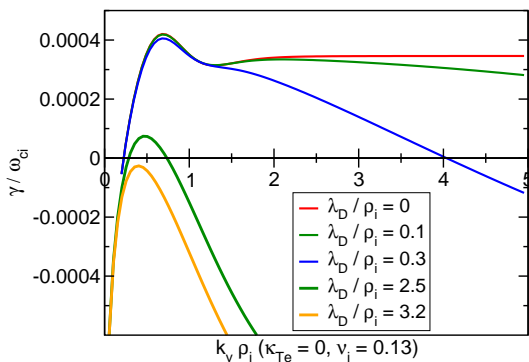


FIGURE 8. ITG mode in a pair plasma with the proton contamination $\nu_i = 0.13$ for $\tau_i = 1$ and $k_{\parallel} \rho_i = 7.4 \times 10^{-4}$. Effects of the finite Debye length is considered.

can have a strongly stabilising effect on the ITG stability, as shown in Fig. 8. One sees that for a given k_{\parallel} , the ITG instability can disappear for all perpendicular wavelengths if λ_D / ρ_i is large enough.

6. ETG instability

Consider now the case when only electron and positron temperature gradients are present, i. e. $\omega_{T(e,p)} \neq 0$, while $\omega_{Ti} = 0$ and $\omega_{*(e,p,i)} = 0$ (flat density). In this Section, we will also allow for unequal temperatures of different species. Therefore, the notation defined in Eq. (5.1) will be used. In this notation, the dispersion relation is

$$1 + k_{\perp}^2 \lambda_D^2 + \sum_{a=p,e} \frac{\hat{\nu}_a}{2} \zeta_a \left[Z_{0a} \Gamma_{0a} + \frac{\omega_{Ta}}{\omega} \left(\frac{3}{2} Z_{0a} \Gamma_{0a} - Z_{0a} \Gamma_{*a} - Z_{2a} \Gamma_{0a} \right) \right] = 0 \quad (6.1)$$

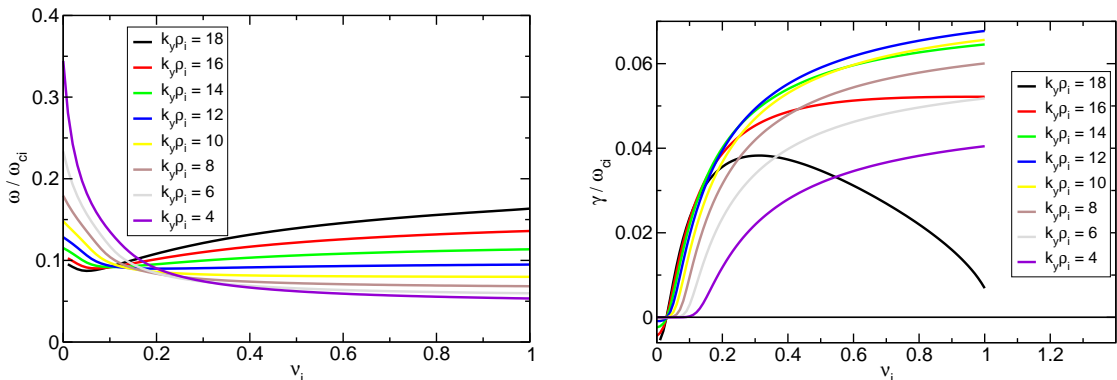


FIGURE 9. Frequency and growth rate of the ETG mode in a three-component electron-positron-proton plasma for $\omega_{Tp} = \omega_{Te}$. One sees that the ion fraction must exceed some threshold for the ETG to be unstable. Here, $k_{\parallel}\rho_i = 7.4 \times 10^{-4}$, $\kappa_{ni} = 0$, $\lambda_D = 0$, and $\tau_a = 1$.

For the perpendicular wave numbers, we assume $k_{\perp}\rho_i \gg 1$ but $k_{\perp}\rho_{(e,p)} \ll 1$. Then

$$\Gamma_{0i} = 0, \quad \Gamma_{*i} = 0, \quad \Gamma_{0(e,p)} = 1, \quad \Gamma_{*(e,p)} = 1 \quad (6.2)$$

Assuming large frequencies $\omega \gg k_{\parallel}v_{\text{th}(e,p)}$, we can write

$$Z_0(\zeta_{e,p}) \approx -\frac{1}{\zeta_{e,p}} - \frac{1}{2\zeta_{e,p}^3} - \frac{3}{4\zeta_{e,p}^5} \quad (6.3)$$

Under these assumptions, the dispersion relation reduces in the leading order to

$$\left(\frac{\hat{\nu}_i}{2} + k_{\perp}^2 \lambda_D^2\right) + \frac{\hat{\nu}_e \tau_e \omega_{Te} + \hat{\nu}_p \tau_p \omega_{Tp}}{4\omega \zeta_e^2} = 0 \quad (6.4)$$

Here, the relations $\sum_a \hat{\nu}_a = 2$ and $\zeta_p^2 = \zeta_e^2 / \tau_p$ have been employed. Let us now consider the case of equal electron and positron temperature profiles, implying $\tau_p = \tau_e = 1$ and $\omega_{Te} + \omega_{Tp} = 0$. Recall that $\tau_a = T_a / T_e$, and our sign conventions imply $\omega_{Te} > 0$ and $\omega_{Tp} < 0$. These conditions are likely since the characteristic time of the energy exchange between the electrons and the positrons is comparable to their Maxwellisation time. If the plasma has had time to reach a locally Maxwellian state, as we have assumed, the electron and positron temperatures should also have equilibrated. Then, the unstable solution is

$$\omega = \frac{1}{2^{1/3}} \left(\frac{k_{\parallel}^2 v_{\text{the}}^2}{\hat{\nu}_i + 2k_{\perp}^2 \lambda_D^2} \hat{\nu}_i \tau_i \omega_{Te} \right)^{1/3} \left(\frac{1}{2} + i \frac{\sqrt{3}}{2} \right) \quad (6.5)$$

This solution corresponds to the fluid limit of the slab ETG instability, which is similar to the ITG instability, Eq. (5.5), but has a frequency of the opposite sign. The mode is expected to be stable in a pure pair plasma $\hat{\nu}_i = 0$, as can indeed be seen from the numerical solution of the full dispersion relation Eq. (2.15), shown in Fig. 9. In Eq. (6.5), however, also the denominator vanishes at $\hat{\nu}_i = 0$ if $k_{\perp}\lambda_D = 0$. This indicates that higher-order terms must be considered in order to address this limit. Also, it indicates sensitivity of the ETG mode in contaminated pair plasmas to finite-Debye-length effects.

Interestingly, the ETG mode can be unstable also in a pure pair plasma ($\hat{\nu}_i = 0$) when the electron and the positron temperature gradients are different for some reason.

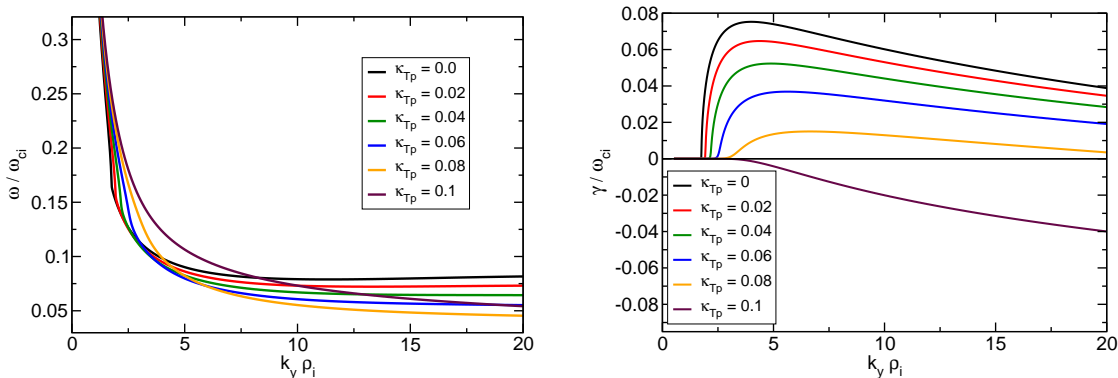


FIGURE 10. Frequency and growth rate of the ETG mode in a pure pair plasma when the symmetry between the species is broken by a difference in the electron and positron temperature profiles. The electron temperature profile with $\kappa_{Te} = 0.1$ is kept fixed. Here, $\lambda_D/\rho_i = 0.1$ and $\tau_a = 1$.

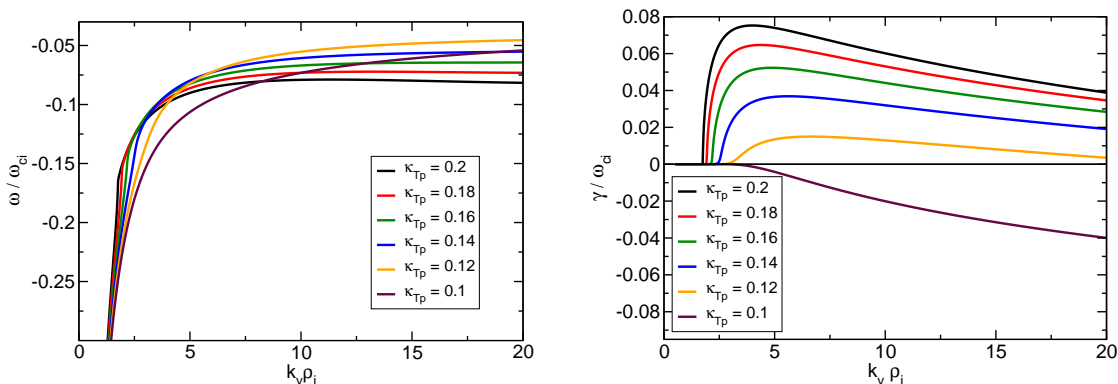


FIGURE 11. Frequency and growth rate of the PTG mode in a pure pair plasma when the symmetry between the species is broken by a difference in the electron and positron temperature profiles. The electron temperature profile with $\kappa_{Te} = 0.1$ is kept fixed. Here, $\lambda_D/\rho_i = 0.1$ and $\tau_a = 1$.

Assuming for simplicity $k_{\perp} \lambda_D$ to be finite, we can write the unstable ETG solution as

$$\omega = \frac{1}{2^{1/3}} \left(\frac{k_{\parallel}^2 v_{the}^2}{k_{\perp}^2 \lambda_D^2} \frac{\tau_e \tau_p}{\tau_e + \tau_p} \left[|\omega_{Te}| - |\omega_{Tp}| \right] \right)^{1/3} \left(\frac{1}{2} + i \frac{\sqrt{3}}{2} \right) \quad (6.6)$$

The numerical solution of the dispersion relation Eq. (2.15) corresponding to a pure pair plasma ETG is shown in Fig. 10. This result is valid if the electrons have a steeper temperature profile. Otherwise, the ETG instability is replaced by the PTG (Positron Temperature Gradient driven) instability, which has a negative frequency:

$$\omega = \frac{1}{2^{1/3}} \left(\frac{k_{\parallel}^2 v_{the}^2}{k_{\perp}^2 \lambda_D^2} \frac{\tau_e \tau_p}{\tau_e + \tau_p} \left[|\omega_{Tp}| - |\omega_{Te}| \right] \right)^{1/3} \left(-\frac{1}{2} + i \frac{\sqrt{3}}{2} \right) \quad (6.7)$$

The PTG solution is shown in Fig. 11.

7. Shear Alfvén wave

Finally, we consider a homogeneous plasma (all profiles are flat) and solve the electromagnetic dispersion relation Eq. (2.15) at finite β . Assuming $k_{\parallel}v_{\text{th}i} \ll \omega \ll k_{\parallel}v_{\text{th}e}$, one can write:

$$Z_{0i} = -\frac{1}{\zeta_i} - \frac{1}{2\zeta_i^3} + \mathcal{O}\left(\frac{1}{\zeta_i^5}\right), \quad Z_{0(e,p)} = i\sqrt{\pi} + \mathcal{O}(\zeta_e) \quad (7.1)$$

$$Z_{1i} = -\frac{1}{2\zeta_i^2} + \mathcal{O}\left(\frac{1}{\zeta_i^4}\right), \quad Z_{1(e,p)} = 1 + \mathcal{O}(\zeta_e) \quad (7.2)$$

$$Z_{2i} = -\frac{1}{2\zeta_i} + \mathcal{O}\left(\frac{1}{\zeta_i^3}\right), \quad Z_{2(e,p)} = \zeta_e + \mathcal{O}(\zeta_e^2) \quad (7.3)$$

For flat profiles $\omega_{*a} = 0$ and $\eta_a = 0$. Hence, from Eq. (2.9)

$$W_{0a} = \zeta_a Z_{0a} \Gamma_{0a}, \quad W_{1a} = \zeta_a Z_{1a} \Gamma_{0a}, \quad W_{2a} = \zeta_a Z_{2a} \Gamma_{0a} \quad (7.4)$$

Employing the appropriate expansions of the plasma dispersion function, we obtain:

$$W_{0i} = -\Gamma_{0i} - \frac{\Gamma_{0i}}{2\zeta_i^2} + \mathcal{O}\left(\frac{1}{\zeta_i^4}\right), \quad W_{0(e,p)} = i\zeta_{e,p}\sqrt{\pi} + \mathcal{O}(\zeta_{e,p}^2) \quad (7.5)$$

$$W_{1i} = -\frac{\Gamma_{0i}}{2\zeta_i} + \mathcal{O}\left(\frac{1}{\zeta_i^3}\right), \quad W_{1(e,p)} = \zeta_{e,p} + \mathcal{O}(\zeta_{e,p}^2) \quad (7.6)$$

$$W_{2i} = -\frac{\Gamma_{0i}}{2} + \mathcal{O}\left(\frac{1}{\zeta_i^2}\right), \quad W_{2(e,p)} = \zeta_{e,p}^2 + \mathcal{O}(\zeta_{e,p}^3) \quad (7.7)$$

For equal temperatures and charges of the species, Eq. (2.15) becomes

$$\begin{aligned} & \left(1 + k_{\perp}^2 \lambda_D^2 + \frac{1}{2} \sum_a \nu_a W_{0a}\right) \left(1 - \sum_a \frac{2\beta_a}{k_{\perp}^2 \rho_a^2} W_{2a}\right) + \\ & + \sum_a \nu_a W_{1a} v_{\text{th}a} \sum_a \frac{\beta_a}{k_{\perp}^2 \rho_a^2} \frac{W_{1a}}{v_{\text{th}a}} = 0 \end{aligned} \quad (7.8)$$

Here, the notation $\beta_a = \mu_0 n_a T_a / B^2$ is used and the usual assumption $\beta_a \ll 1$ is made. We will substitute the approximate expressions for W_{na} , derived above, into this dispersion relation. Note that small terms of the order $1/\zeta_i^2$ and $1/\zeta_i$ must be kept in W_{0i} and W_{1i} , respectively, since they give order unity contributions in the dispersion relation when multiplied with ζ_e^2 appearing in $W_{2(e,p)}$ and $W_{1(e,p)}^2$. For equal temperatures and charges of the species, one can write:

$$\frac{\zeta_e^2}{\rho_e^2} = \frac{\zeta_i^2}{\rho_i^2}, \quad \zeta_e v_{\text{th}e} = \zeta_i v_{\text{th}i}, \quad \beta_a = \nu_a \beta_e, \quad \nu_i + \nu_p = 1 \quad (7.9)$$

Using these relations and assuming $k_{\parallel}v_{\text{th}i} \ll \omega \ll k_{\parallel}v_{\text{th}e}$, one can write the dispersion relation to the lowest order as follows:

$$\begin{aligned} & \left(1 + k_{\perp}^2 \lambda_D^2 - \frac{\nu_i \Gamma_{0i}}{2}\right) \left[1 - \frac{2\beta_e \zeta_e^2 (1 + \nu_p)}{k_{\perp}^2 \rho_e^2}\right] + (1 + \nu_p)^2 \frac{\beta_e \zeta_e^2}{k_{\perp}^2 \rho_e^2} + \\ & + \frac{\nu_i \beta_e \Gamma_{0i}}{k_{\perp}^2 \rho_i^2} \left[\frac{\nu_i}{2} (1 - \Gamma_{0i}) + k_{\perp}^2 \lambda_D^2\right] = 0 \end{aligned} \quad (7.10)$$

For conventional plasmas with $\nu_i = 1$ and $\nu_p = 0$, and the long-wavelength approximation for Γ_{0i} , this dispersion relation reduces to the shear Alfvén wave (SAW):

$$2\beta_e\zeta_i^2 = 1 \Leftrightarrow \omega^2 = k_{\parallel}^2 \frac{B^2}{\mu_0 m_i n_{0e}} = k_{\parallel}^2 v_A^2 \equiv \omega_A^2 \quad (7.11)$$

For a finite positron fraction, one can write

$$2\beta_e\zeta_i^2 = \frac{1}{\nu_i} \frac{2 - \nu_i \Gamma_{0i} + \mathcal{O}(\beta_e)}{2 - \nu_i} \frac{k_{\perp}^2 \rho_i^2}{1 - \Gamma_{0i}} \quad (7.12)$$

if the Debye length is neglected. In the long-wavelength approximation

$$2\beta_e\zeta_i^2 = \frac{1}{\nu_i} \Leftrightarrow \omega = \omega_A / \sqrt{\nu_i} = k_{\parallel} \frac{B}{\sqrt{\mu_0 m_i n_{0i}}} = k_{\parallel}^2 v_{Ai}^2 \equiv \omega_{Ai} \quad (7.13)$$

The numerical solution of the full dispersion relation Eq. (2.15) for the shear Alfvén wave parameters is shown in Fig. 12. One sees, as expected, that the frequency of the shear Alfvén wave increases very rapidly when $\nu_i \rightarrow 0$ (note the logarithmic scale in the Figure), in agreement with our findings and Helander & Connor (2016).

Note that Eq. (7.13) highlights the role of the ions, which carry most of the plasma inertia even at small ν_i , but it is singular for $\nu_i = 0$. This formal singularity can be resolved taking the finite Debye length into account. In the long-wavelength approximation

$$2\beta_e\zeta_i^2 = \frac{2 - \nu_i + 2k_{\perp}^2 \lambda_D^2}{\nu_i k_{\perp}^2 \rho_i^2 + 2k_{\perp}^2 \lambda_D^2} \frac{k_{\perp}^2 \rho_i^2}{2 - \nu_i} = \frac{1}{\nu_i + 2\lambda_D^2 / \rho_i^2} [1 + \mathcal{O}(k_{\perp}^2 \lambda_D^2)] \quad (7.14)$$

This equation describes coupling of the “ion shear Alfvén wave”, based on ion inertia, to a wave travelling at the speed of light (Zocco 2017). Indeed, in a pure pair plasma, the dispersion relation Eq. (7.14) reduces for small $k_{\perp} \lambda_D < 1$ to

$$\omega^2 = k_{\parallel}^2 \frac{B^2}{\mu_0 m_e n_{0e}} \frac{\rho_e^2}{2\lambda_D^2} \Leftrightarrow \omega = k_{\parallel} c \quad (7.15)$$

As shown in Fig. 12, the shear Alfvén wave (SAW) transforms for $\nu_i \rightarrow 0$ into the electromagnetic wave, for which the displacement current must be taken into account in order to address it properly, see (Zocco 2017) for details. For large $k_{\perp} \lambda_D > 1$, a whistler-type solution $\omega \sim k^2$ is obtained:

$$2\beta_e\zeta_e^2 = \frac{k_{\perp}^2 \rho_e^2}{2} \Leftrightarrow \omega = \frac{1}{2} \frac{k_{\perp} \rho_e}{\sqrt{\beta_e}} k_{\parallel} v_{the} \quad (7.16)$$

This whistler-type wave can be found also in conventional plasmas and proton-contaminated pair plasmas, as shown in Fig. 13, where the dispersion relation Eq. (2.15) is solved numerically. The transitions between the shear Alfvén wave, electromagnetic wave, and the whistler can be seen clearly.

8. Conclusions

In this paper, we have studied the gyrokinetic stability of pair plasmas solving the dispersion relation (2.15) analytically and numerically. It is found that pair plasmas can support the gyrokinetic ITG, ETG and universal instabilities even in slab geometry if the proton fraction exceeds some threshold. In practice, however, this threshold is usually quite large, hopefully large enough to keep the proton content below this value in pair plasma experiments (Pedersen *et al.* 2012). These results extend the finding of Helander (2014) that pair plasmas are stable to gyrokinetic modes in the absence of magnetic

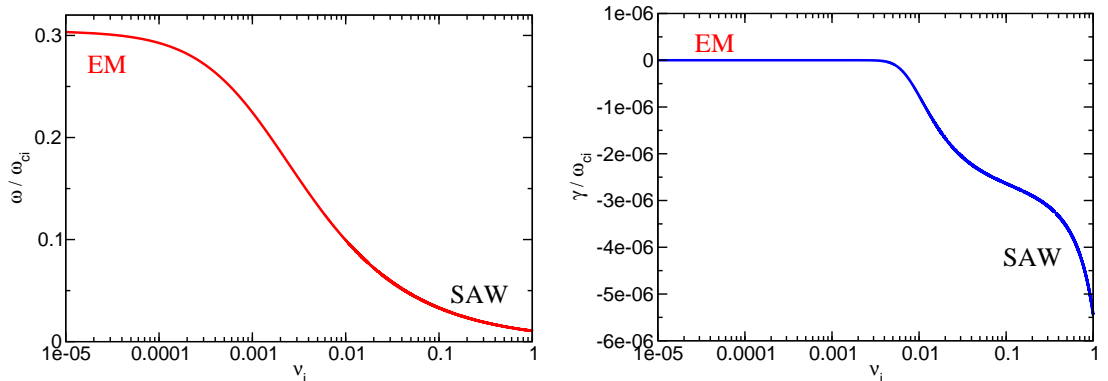


FIGURE 12. Frequency and growth rate of the shear Alfvén wave (SAW) as a function of ion contamination in a pair plasma for $k_{\perp} \rho_i = 0.05$, $k_{\parallel} \rho_i = 7.4 \times 10^{-4}$, $\lambda_D / \rho_i = 0.01$, and $\beta_e = 0.005$. One sees the transition from the SAW regime $\nu_i \sim 1$ to a regime of an electromagnetic wave travelling at the speed of light when $\nu_i \rightarrow 0$. The latter limit is not properly described by the gyrokinetic theory of this paper since the relativistic effects must be taken into account in the wave dynamics (Zocco 2017).

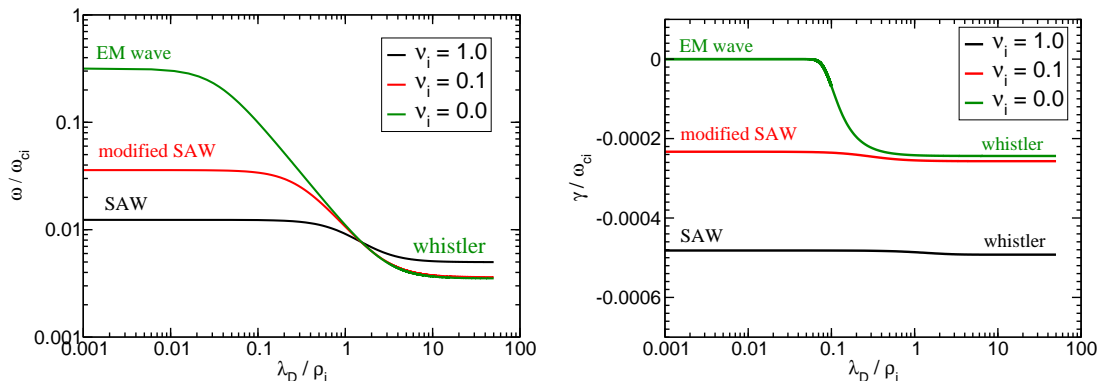


FIGURE 13. Frequency and growth rate of the shear Alfvén wave (SAW), “whistler” and electromagnetic (EM) wave as a function of the Debye length in a conventional plasma, proton-contaminated pair plasma and pure pair plasma. Transitions between different regimes are clearly seen. The parameters used are $k_{\perp} \rho_i = 0.475$, $k_{\parallel} \rho_i = 7.4 \times 10^{-4}$, and $\beta_e = 0.005$. Note that $\lambda_D \gtrsim \rho_e / \sqrt{\beta_e}$ implies $v_{the} \gtrsim c$. This case is not properly described by the gyrokinetic theory of this paper since relativistic effects must be taken into account in the particle dynamics (Zocco 2017).

curvature to the cases with small to moderate proton contamination. We find, however, that pure pair plasmas can have temperature-gradient-driven instabilities, if the electron and the positron temperature profiles differ. In reality, however, such profiles are unlikely in steady state, since the characteristic time of energy exchange between the species is comparable to the Maxwellisation time. In the electromagnetic regime, we find that the shear Alfvén wave is present in a contaminated plasma. Its frequency increases very rapidly when the ion fraction becomes negligible.

Acknowledgements We acknowledge Thomas Sunn Pedersen and PAX/APEX experiment team for their interest to our work. A. M. thanks V. S. Mikhailenko and V. D. Yegorenkov for bringing his attention to the K-mode solutions of kinetic dispersion relations. R. Kleiber is acknowledged for providing a module for a numerical root finding.

REFERENCES

- CARPENTIER, M. P. & SANTOS, A. F. D. 1982 Solution of equations involving analytic functions. *Journ. Comp. Phys.* **45**, 210–220.
- COPPI, B., ROSENBLUTH, M. N. & SAGDEEV, R. Z. 1967 Instabilities due to temperature gradients in complex magnetic field configurations. *Phys. Fluids* **10**, 582–587.
- DAVIES, B. 1986 Locating the zeros of an analytic function. *Journ. Comp. Phys.* **66**, 36–49.
- FRIED, B. & GOULD, R. 1961 Longitudinal ion oscillations in a hot plasma. *Phys. Fluids* **4** (1), 139–147.
- HELANDER, P. 2014 Microinstability of magnetically confined electron-positron plasmas. *Phys. Rev. Lett.* **113**, 135003+4.
- HELANDER, P. & CONNOR, J. 2016 Gyrokinetic stability theory of electron-positron plasmas. *J. Plasma Phys.* **82**, 9058203+13.
- PEDERSEN, T., BOOZER, A., DORLAND, W., KREMER, J. & SCHMITT, R. 2003 Prospects for the creation of positron-electron plasmas in a non-neutral stellarator. *J. Phys B: At. Mol. Opt. Phys.* **36**, 1029–1039.
- PEDERSEN, T., DANIELSON, J., HUGENSCHMIDT, C., MARX, G., SARASOLA, X., SCHAUER, F., SCHWEIKHARD, L., SURKO, C. & WINKLER, E. 2012 Plans for the creation and studies of electronpositron plasmas in a stellarator. *New J. Phys.* **14**, 03510+13.
- SAITOH, H., STANJA, J., STENSON, E., HERGENHAHN, U., NIEMANN, H., PEDERSEN, T., STONEKING, M., PIOCHACZ, C. & HUGENSCHMIDT, C. 2015 Efficient injection of an intense positron beam into a dipole magnetic field. *New J. Phys.* **17**, 103038+9.
- YEGORENKOV, V. & STEPANOV, K. 1987 *Dop. Akademii Nauk URSS, Ser. A* (8), 44.
- YEGORENKOV, V. & STEPANOV, K. 1988 *JETP* **94**, 116.
- ZOCCO, A. 2017 Slab magnetised non-relativistic low-beta electron-positron plasmas: collisionless heating, linear waves and reconnecting instabilities. *Submitted to Journal of Plasma Physics* .